Design analysis of a decentralized equilibrium-routing strategy for intelligent vehicles

Mahajan, Niharika; Hegyi, Andreas; Hoogendoorn, Serge P.; van Arem, Bart

DOI
10.1016/j.trc.2019.03.028

Publication date
2019

Document Version
Final published version

Published in
Transportation Research Part C: Emerging Technologies

Transportation Research Part C 103 (2019) 308–327

Contents lists available at ScienceDirect

Transportation Research Part C

journal homepage: www.elsevier.com/locate/trc

Design analysis of a decentralized equilibrium-routing strategy for intelligent vehicles☆

Niharika Mahajan*, Andreas Hegyi, Serge P. Hoogendoorn, Bart van Arem

Delft University of Technology, Faculty of Civil Engineering and Geosciences, Department of Transport & Planning, Stevinweg 1, 2628 CN Delft, the Netherlands

ARTICLE INFO

Keywords:
Control design
In-vehicle routing
Decentralized predictive routing
User-equilibrium routing
Traffic prediction using neural networks
Intelligent vehicles

ABSTRACT

Intelligent vehicle technologies are opening new possibilities for decentralized vehicle routing systems, suitable for regulating large traffic networks, and at the same time, capable of providing customized advice to individual vehicles. In this study, we perform a rigorous simulation-based analysis of an in-vehicle routing strategy that aims to achieve a user-equilibrium distribution in traffic. Novel features of the approach include: a mechanism based on forward propagation of individual vehicle decisions to anticipate future traffic dynamics; time-dependent prediction of route travel times with neural network-based link predictors; and a stochastic routing policy for in-vehicle decision-making based on predicted travel times. However, for an effective application of the approach, design choices need to be made regarding the accuracy of the link predictors, and some control settings. These choices may depend on the network size and structure. We investigate the impact of two important design aspects: sequentially using link-level predictors for route travel time estimation, and the control parameter values, on the equilibrium performance at the network-level. The results suggest functional scalability of the approach, in terms of the prediction model accuracy and routing performance. Overall, the work contributes to a qualitative and quantitative understanding of emergent performance from the given routing approach.

1. Introduction

Dynamic route guidance in freeway or urban traffic networks with time-varying demand and stochastic travel times is a classic transportation problem (Papageorgiou, 1990). At the same time, recent advances in automated and connected vehicle capabilities (Shladover, 2017), boosted by other emerging technologies, like cloud computing, artificial intelligence, big data, and internet of things, are fundamentally transforming the potential and design of traffic control systems (Diakaki et al., 2015; Papageorgiou et al., 2015). In-vehicle route guidance systems, be they satellite navigation devices or GPS enabled smartphone applications, such as Google Maps, Waze, and Apple Maps, are becoming ubiquitous and connected. These trends are making decentralized routing approaches increasingly more practicable. The benefits of a decentralized control structure range from lower computation and communication loads, higher fault tolerance, to robustness against measurement errors, delays and failures. Moreover, decentralized decision-making makes it possible to provide personalized advice to individual vehicles. We focus on decentralized route guidance systems that can achieve a user-equilibrium (UE) condition, famously known as the Wardrop's first principle of route choice

☆ This article belongs to the Virtual Special Issue on "CAV Control".

* Corresponding author.
E-mail addresses: n.mahajan@tudelft.nl (N. Mahajan), a.hegyi@tudelft.nl (A. Hegyi), s.p.hoogendoorn@tudelft.nl (S.P. Hoogendoorn), b.vanarem@tudelft.nl (B. van Arem).

https://doi.org/10.1016/j.trc.2019.03.028
Received 28 February 2018; Received in revised form 19 March 2019; Accepted 31 March 2019
Available online 28 April 2019
0968-090X/

(Wardrop, 1952). UE routing entails reallocating vehicle flows in a way that individual travel time costs are minimized, and cannot be further decreased by unilateral action. Not just is a UE optimal for individual users, it also results in a fair distribution, wherein all vehicles over all used routes between an origin-destination (OD) experience equal travel times.

In this work, we study the design aspects of a cooperative route guidance system proposed by Claes (2015) for UE routing of individual vehicles. The investigated strategy uses a decentralized predictive algorithm, wherein the prediction model is decentralized at the level of individual links, and the routing decisions are decentralized at the level of individual vehicles. Central to its design is a coordination mechanism that does not use direct vehicle-to-vehicle communication. Instead, intelligent vehicles (IVs) cooperate by delegating virtual agents to share their planned (future) routes with roadside agents, which are computation and communication devices deployed across links in the physical network. These roadside agents constitute the environment that records information of individual route plans, and aggregate it to estimate time-dependent travel times. The vehicles can thereafter use the predictions to update their future routing plans. In this way, by integrating the travel time prediction and routing models, not just the current traffic condition but also the control decisions can be included in the predictions.

An effective implementation of the approach depends on the understanding of some important design aspects. First, the time-dependent route travel time predictions are made in a decentralized model using multiple Artificial Neural Network (ANN)-based link predictors. Individual link predictors estimate link travel times using local in-vehicle information. These link predictions are then aggregated to estimate route travel times. The issue however is that the errors in link estimates may negatively impact the prediction accuracy of subsequent link predictors. Thus, the propagation of error over multiple links determines the reliability of the route travel time predictions. How the link and route travel time accuracy relate, is moreover valuable for identifying a design criterion for the link predictor accuracy. Next, individual vehicles instantaneously react to these predictions using a stochastic routing decision-criterion. This is unlike model-predictive type control where the control signal is explicitly optimized over a future horizon. The routing behavior thus achieved depends on the choice of two control parameters – one of which influences the responsiveness of the routing decision to the travel time difference between the chosen and the fastest alternatives, and the other specifies the frequency of decision update. Tuning these control parameters requires identifying mechanisms and quantities that reflect the impact of the parameter values on the system performance. We study the discussed design aspects using systematic simulations, making the following research contributions:

1. Evaluating error propagation over multiple link predictors and its impact on the accuracy of route travel time estimates.
2. Evaluating the influence of control settings on control stability and on the internal (predicted) and external (actual) performance of the routing system.
3. Analyzing the emergent dynamics towards UE in 3 different network topologies.

The above contributions are motivated towards understanding the operational requirements, and overall scalability of the presented routing system. Aspects related to the design, like prediction methodology, tunable parameters, are important determinants of scalability, which we focus on in this work. At the same time, the available communication and computation technologies (their load capacity, delay and loss behavior) are other relevant aspects, which we only briefly discuss. Similar to our analysis of the control design aspects, the latter technological aspects require an in-depth study of their own.

The remainder of the article is structured as follows. Section 2 positions the work in context of related literature. Section 3 describes the workings of the route guidance system. Next, the system characteristics are analyzed qualitatively in Section 4, and quantitatively (by means of simulations) in Section 5. Finally, the conclusions and recommendations of this research are presented in Section 6.

2. Background

Present-day navigation systems rely primarily on historic or (near-) instantaneous travel time measurements. This is in part due to the high latency of loop detector data, and the lack of efficient network-scale prediction algorithms. The routing behavior thus achieved is that of congestion avoidance, since the system can only react after a congestion has been detected. As a result, the effects of routing advice become evident at a bottleneck location with some delay. Such systems also suffer from the overreaction phenomenon (Ben-Akiva et al., 1991). Overreaction occurs when majority of the users, failing to consider the response of other users, react similarly to the current traffic situation/information, resulting in the congestion to transfer from one route to another. Predictive strategies that make future control decisions based on a forecast of the traffic evolution ensure better performance.

Predictive optimization-based strategies, more commonly known as Model Predictive Control (MPC), are known to perform optimally with respect to the employed traffic model (Hegyi et al., 2005a; Hegyi et al., 2005b; Hajiahmadi et al., 2013). By finding the optimal control signal over a future horizon, these approaches successfully include lag effects, i.e the delay between the time control decisions are made and when their effects become evident in more downstream locations. The lag effects can be particularly significant in large traffic networks, making MPC a superior choice compared to more simple feedback policies. Moreover, performance in an MPC approach is assured as long as disturbances are predictable, demand pattern is known, and the prediction model represents the traffic dynamics accurately. Still, the practical challenge in using these strategies is their high computational demand, from using complex prediction models and solving a large non-linear optimization problem in real-time.

Predictive feedback strategies are different from sophisticated MPC controllers, as they do not the control signal is not optimized over a future horizon. Instead, the controller generates a reactive control decision based on the predictions of the traffic state or select measurement variables. These approaches (Messmer et al., 1998; Wang et al., 2003) have gained interest, especially for real-time

application, as they combine the ease of application of feedback controllers (Pavlis and Papageorgiou, 1999; Wang et al., 2001; Wang et al., 2006) with the performance benefits of considering future effects without having to use complex optimization models. The predictive feedback routing strategy described in Wang et al. (2003) is decentralized to some extent, as each decision node in the network uses the feedback policy to update destination-specific splitting fractions. Furthermore, in a simulation-based evaluation, the authors show that for networks with long links (where lag effects dominate), their predictive feedback policy is an improvement over simple feedback policies, while being computationally less demanding compared to model-based iterative strategies.

Fully decentralized predictive approaches like in Claes et al. (2011), Du et al. (2014), where the routing decisions are made at the level of individual vehicles based on traffic state predictions, are even more relevant for intelligent vehicle systems. There are multiple advantages of vehicle-level decision-making. First, the routing system can utilize vehicle-specific information into the control logic. The information can be: operational, related to an individual vehicle's destination and planned route (Claes et al., 2011; Du et al., 2014); characteristic information about the vehicle or user (Adler et al., 2005; Pang et al., 1999; Wahle et al., 2001); or behavioral information about a vehicle's routing decisions in the past. Second, on-board computation capacity can be better leveraged. Finally, in-vehicle routing systems can also be used to incentivize cooperation between vehicles (Helbing et al., 2005; Kato et al., 2002). However, more common in literature are decentralized approaches that use instantaneous traffic information (Grzybek et al., 2015). Such systems are commonly designed as multi-agent systems, employing nature-inspired metaheuristic algorithms (Cong et al., 2013) or game theoretic principles (Klein and Ben-Elia, 2016; Garcia et al., 2000) for optimization. The important feature of such multi-agent systems is that even though agents themselves keep limited knowledge of the system, and have limited capacity to individually achieve the overall objective (Jennings et al., 1998), system-level behavior emerges from the many local non-linear interactions between the agents (individual vehicles), and between agents and the environment (the traffic network).

The contribution by Weyns et al. (2007) was to conceptualize an ant colony inspired decentralized approach that uses predictive traffic information within a multi-agent framework. The strategy was later developed and shown to effectively reach dynamic user-equilibrium in city-scale networks, even when 40% of all vehicles are controlled (Claes et al., 2011; Claes, 2015).

We further Claes' work by identifying and examining the internal mechanisms that drive the emergent control response. The overall aim is to learn about the requirements towards a practical application of the decentralized routing approach. We study how the different design aspects influence control behavior, and how the resulting design requirements may depend on the network size. Even though we examine the strategy in simple networks with a single origin-destination, the methodology adopted in our analysis is transferable to larger networks. In that sense, our work is a first step towards evaluating the scalability of a promising decentralized vehicle route guidance system.

3. Decentralized in-vehicle routing

This section details the decentralized in-vehicle routing strategy investigated in this work. The objective of the routing strategy is to utilize in-vehicle information, and present-day computation and communication infrastructures, to achieve a user-equilibrium routing in a decentralized framework where each individual user makes independent routing decisions based on traffic predictions. The strategy is in principle based on the work of Claes (2015). However, this paper presents the following new design contributions: (i) describing the logical components of the strategy from a traffic theoretic viewpoint, (ii) adding inputs to the neural network-based link predictors that can better describe spillback effects, and include desired speed differences between vehicles, and (iii) using a correction for predictions made for the link a vehicle currently occupies. In the remainder section, we first describe the system architecture at a high-level, and then elaborate the workings of the routing and prediction approaches.

3.1. Multi-agent based system design

The routing strategy uses a multi-agent architecture to distribute tasks between multiple agents that interact to achieve a collective objective, which could not have been accomplished by any of the agents alone. The collective objective here is to achieve user-equilibrium routing assignment of IVs. Agents in multi-agent systems can be autonomous physical or software entities that make decisions, communicate and trigger other agents to act in response to dynamic changes in their environment. The routing strategy employs two different agents, namely *vehicle agents* and *link agents*. The vehicle and link agents are seated in physical infrastructure; a vehicle agent resides on the on-board computer in an IV, and a link agent on a roadside electronic device that is capable of computation and communication with other agents. The vehicle agent furthermore employs two delegate or sub-agents: *exploration* and *intention agents*. These delegate agents are virtual agents that facilitate communication between the vehicle and link agents, similar to the role of pheromone in ant foraging type algorithms. The agents use a map of the network to identify the link agents associated to different road sections. The vehicle and link agents interact iteratively, using each other's information as feedback for subsequent actions. Fig. 1 gives a high-level illustration of the interaction between a single vehicle and link agent. The core functions of these agents are as follows:

- *Vehicle Agent* (i) delegates an *intention agent* to communicate its current route plans to link agents along the chosen route, (ii) delegates multiple *exploration agents*, one per candidate route, to sequentially traverse link agents along a given route, and in the end return the predicted route travel time to the vehicle agent, and (iii) updates its route decision based on the route travel time estimates provided by the exploration agents.
- *Link Agent* (i) keeps record of the future link occupancy based on the individual route plans reported by the intention agents, and (ii) provides travel time prediction for their link when requested for by an exploration agent. Travel time predictions are time-specific, which means that a prediction is made for the specific time that a vehicle expects to enter a link.

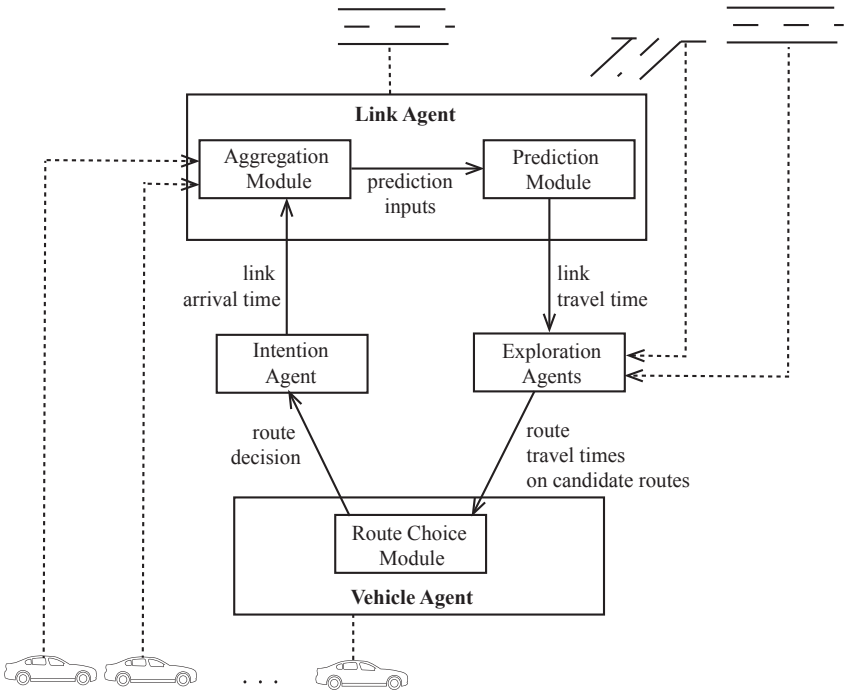

Fig. 1. Interaction between agents in the multi-agent framework. The solid arrows indicate the main information exchange between the agents, and the dotted arrows indicate equivalent information as obtained from other vehicle and link agents in the network.

3.2. Notation

The transport network is defined as a graph with a set of nodes and directed links, where each link represents a physical road section and its corresponding roadside unit. The set of all routes in the network is R, and I_r is the sequence of all links on a route $r \in R$. N is a sequence of all vehicles in the network, sorted in increasing order by their network entry times. A vehicle $n \in N$ exploring a candidate route $r \in R$, is additionally described by a sequence of links of $I_{n,r} = (i_1, i_2, ..., i_m, ..., i_M)$ that the given vehicle is yet to traverse along the route. Here, i_1 denotes the vehicle's current link, i_m the m^{th} link along its remainder path, and i_M its destination link.

An *intention* is defined as a planned route decision that a given vehicle is assumed to adhere to, unless updated with a new advice. Route intention of a vehicle n along a route r is recorded as a sequence of link arrival times $(t^{\text{arr}}_{n,i_1}, t^{\text{arr}}_{n,i_2}, ..., t^{\text{arr}}_{n,i_m}, ..., t^{\text{arr}}_{n,i_M})$, where each element corresponds respectively to the expected arrival times for links in $I_{n,r}$.

The control system uses a time step index $k \in \mathbb{N}$, for a time interval $[kT, (k+1)T)$, where T is the control time step size, i.e. the time interval after which a vehicle re-evaluates its routing decision. Similarly, the prediction model uses a time step size $\widetilde{T}$ for discretization, and a time step index $\widetilde{k} \in \mathbb{N}$ denoting a time interval $[\widetilde{k}\widetilde{T}, (\widetilde{k}+1)\widetilde{T})$. Note that these time steps for the prediction and the control system are a design choice and can be different.

All travel time related notations are represented in the form τ^*_*, where the superscript can either be L for a link, or R for a route estimate. The subscript denotes the specific link or route element to which the value corresponds. Furthermore, an additional hat over the symbol: $\hat{\tau}^*_*$, indicates a prediction instead of an experienced travel time.

All predictions are time-dependent in two ways – one, the estimates are provided for a vehicle's anticipated time of arrival, and two, the predictions can be based on intentions collected at any previous time instant. Thus, a vehicle n expecting to arrive on link m at time t^{arr}_{n,i_m} may receive a travel time estimate $\hat{\tau}^{\text{L}}_{i_m}(\widetilde{k}, k)$, where the time-step index $\widetilde{k}$ corresponds to its link arrival time, such that $t^{\text{arr}}_{n,i_m}(k) \in [\widetilde{k}\widetilde{T}, (\widetilde{k}+1)\widetilde{T})$, and the time-step index k is for time kT when the intentions on which the predictions are based were collected. We assume that the latest intention information is available to all link predictors, and thus, for notational simplicity we will drop the second time index k in the rest of the article.

3.3. Routing strategy

In this section, we explain how the different agents perform their respective tasks in order to collectively achieve an equilibrium distribution of traffic. The methodological description in this section is presented from the viewpoint of an individual IV, and includes the (not strictly sequential) functional steps involved in re-evaluating a vehicle's control decision in a given control time-step.

3.3.1. Vehicle agents select a route

A vehicle agent selects its route based on the most recent route travel time prediction it has received. The routing decision uses a

probabilistic criterion, same as in Claes (2015). In comparison to utility-based route choice models, which generally employ a deterministic policy based on a threshold for utility gain (Mahmassani and Jayakrishnan, 1991), our policy determines a probability of switching to a better alternative based on the magnitude of potential gain. The switching probability p is determined by comparing predicted travel times on the last confirmed route r and the fastest available route r^* as:

$$p = 1 - \exp\left(-\alpha\left(\frac{\hat{\tau}^{\mathrm{R}}_{n,r}}{\hat{\tau}^{\mathrm{R}}_{n,r^*}} - 1\right)\right). \tag{1}$$

The resulting behavior is such that the larger the travel time gain from switching to the fastest route is, the larger is the probability of a vehicle updating its intention.

The switching probability function in (1) uses a parameter α, which can be tuned to influence the likelihood of a vehicle agent re-routing to a better alternative. For a given travel time gain, a higher α value improves the chances of a vehicle agent accepting the better route as compared to a lower α value. For instance, for an α value of 25, there is an approximately 70% probability ($p = 0.7$) of rerouting to an alternative which is 5% faster than a vehicle's current route. The influence of the parameter choice is elaborated further in Section 4.2.

3.3.2. Vehicle-intention agents propagate route intentions

Having selected a route, the vehicle agent delegates an *intention agent* to inform relevant link agents of its future arrival. The propagation of the route intentions starts with the link agent corresponding to the link that a vehicle currently occupies. The intention agent then traces the selected route, sequentially informing link agents along the path of its expected arrival and departure times for the link. Furthermore, when a vehicle changes its route intention, it also propagates an intention agent along the previously chosen route to cancel its intended route plan. In this way, by confirmation and cancellation of future intentions, the link agents can accurately maintain intentions of all vehicles that are expected to traverse it. In order to initialize the intentions at the start of control, we use free-flow travel times on the vehicle routes as available from any on board navigation service.

3.3.3. Link agents predict link occupancy function

The intentions from a control time step k inform the travel time predictions in time step $k + 1$. We assume that all link agents can receive intentions from all vehicles in the network (intending to use a given link) within a control interval T. Then, the link agents aggregate these vehicle intentions (which stores information of vehicle arrivals and departures) to maintain cumulative link inflow $N^{\mathrm{arr}}(\widetilde{k})$ and cumulative outflow $N^{\mathrm{dep}}(\widetilde{k})$ information. The occupancy function of a link (i.e. the total number of vehicles on a link at a given time) is therefore available to its link agent, as shown in Fig. 2a. Fig. 2b illustrates how the cumulative curves are discretized for the discretization time step $\widetilde{T}$ with index $\widetilde{k}$. A discrete occupancy function is computed from the discretized cumulative curves as:

$$w_{i_m}(\widetilde{k}) = N^{\mathrm{arr}}(\widetilde{k}) - N^{\mathrm{dep}}(\widetilde{k}). \tag{2}$$

3.3.4. Vehicle-exploration agents explore candidate routes

To ensure that the vehicle agent can update its route in response to changing traffic dynamics, it delegates *exploration agents* to evaluate the routes at a regular intervals of T. Each exploration agent collects information about the vehicle's expected route travel time $\hat{\tau}^{\mathrm{R}}_{n,r}(k)$ along a route r. The set of candidate routes to be explored can be determined using k-shortest path algorithm (based on known free-flow travel times), or any other route-set generation algorithm.

The exploration agent relays link arrival information along links $i_m \in I_{n,r}$ on a route r. Each link agent updates the message with the expected arrival time at the subsequent link in an iterative update:

$$t^{\mathrm{arr}}_{n,i_{m+1}} = t^{\mathrm{dep}}_{n,i_m} = t^{\mathrm{arr}}_{n,i_m} + \hat{\tau}^{\mathrm{L}}_{i_m}. \tag{3}$$

The initial condition for t^{arr}_{n,i_1} equals the time that a vehicle entered the link that it currently occupies at time kT. The process continues until the message arrives at the destination link i_M, where the message is updated to return the expected route travel time $\hat{\tau}^{\mathrm{R}}_{n,r}$:

$$\hat{\tau}^{\mathrm{R}}_{n,r}(k) = t^{\mathrm{arr}}_{n,i_M} + \hat{\tau}^{\mathrm{L}}_{i_M} - kT. \tag{4}$$

These explorations rely on travel time predictions provided by link agents, beginning with the vehicle's current link. For such a link i_1, the link arrival time is known to the vehicle from its geo-spatial positioning system. Let us denote the vehicle arrival time on a given link as $t^{\mathrm{arr}}_{n,i_m} = \bar{k}\widetilde{T}$, and the current time as $\bar{k}\widetilde{T} = kT$; $\bar{k} > \widetilde{k}$ only for the first link i_1. We denote the difference between the current time and the vehicle arrival time as $\Delta t = (\bar{k} - \widetilde{k})\widetilde{T}$. The neural network based link predictors are used to estimate the link travel times $\hat{\tau}^{\mathrm{L,nn}}_{i_m}$ for a specific arrival time. However, for link i_1 the prediction based on the arrival time t^{arr}_{n,i_m} can be inaccurate, because such a prediction ignores the traffic dynamics during the time period Δt that the vehicle has been traveling on the link. This prediction error can be significant, especially when the link is in congested traffic regime (with unstable dynamics). As a correction for such errors, we additionally determine a conservative travel time estimate based on the average of the vehicle's current and desired speeds. The general formulation for the travel time estimate on a given link is as below:

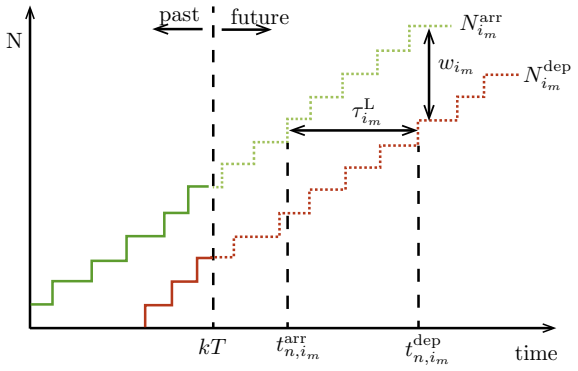

(a) Occupancy function based on actual vehicle arrivals and departures.

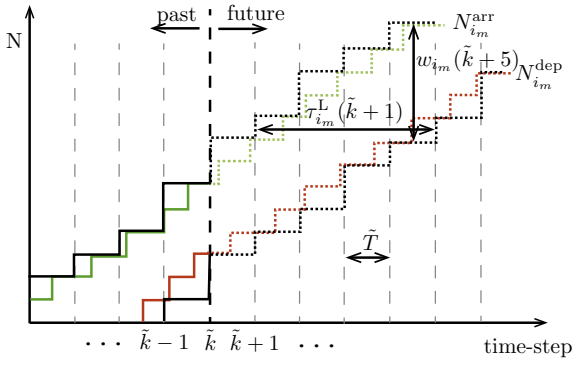

(b) Discretized occupancy function (in black) using a discretization time-step $\tilde{T}$.

Fig. 2. Relation between the link occupancy function and cumulative curves. The solid lines represent historic information, and the dotted lines predicted cumulative curves.

$$\hat{\tau}^{\text{L}}_{i_m}(\tilde{k}) = \begin{cases} \max\left(\hat{\tau}^{\text{L,nn}}_{i_m}(\tilde{k}),\ \Delta t + \frac{X_{i_m} - x}{\frac{v^{\text{des}} + v^{\text{cur}}}{2}}\right), & \text{if } m = 1 \\ \hat{\tau}^{\text{L,nn}}_{i_m}(\tilde{k}), & \text{otherwise.} \end{cases} \tag{5}$$

Here, the X_{i_m} is the total length of link i_m, x the distance travelled on the link, and v^{des} and v^{cur} are the vehicle's desired and current speeds, respectively.

In general, the future link travel time $\hat{\tau}^{\text{L,nn}}_{i_m}(\tilde{k})$ on a link i_m, for an estimated arrival in time-step $\tilde{k}$, can be predicted with a neural network based predictor as

$$\hat{\tau}^{\text{L,nn}}_{i_m}(\tilde{k}) = f(\mathbf{x}(\tilde{\mathbf{k}})). \tag{6}$$

Here, function f represents a neural network-based travel time prediction model. The neural network architecture is discussed in Section 3.4. The input vector $\mathbf{x}(\tilde{\mathbf{k}})$ is given as

$$\mathbf{x}(\tilde{\mathbf{k}}) = \begin{bmatrix} w_{i_m}(\tilde{k}_1) \\ w_{i_m}(\tilde{k}_2) \\ w_{i_m}(\tilde{k}_3) \\ w_{i_m}(\tilde{k}_4) \\ w_{i_m}(\tilde{k}_5) \\ w_{i_{m+1}}(\tilde{k}_1) \\ \vdots \\ w_{i_{m+d}}(\tilde{k}_1) \\ v^{\text{des}}_n \end{bmatrix}, \tag{7}$$

where,

$$\widetilde{k}_j = \left\lfloor \frac{t_j}{\widetilde{T}} \right\rfloor \text{ with } j = 1,\ 2,\ \ldots, 5. \tag{8}$$

The choice of 5 look-back steps is arbitrary, and the same as in Claes (2015). Further, $w_{i_m}(\widetilde{k})$ denote the link occupancy at time $\widetilde{k}\widetilde{T}$, defined as the total number of vehicles on a link at a given time. Similarly, $w_{i_{m+1}}(\widetilde{k}),\ \ldots, w_{i_{m+d}}(\widetilde{k})$ are the link occupancies of the d directly downstream links (2 or more in case of a diverge) at the same time index. The last element of (7) is the desired speed v_n^{des} of the predicting vehicle n, easily available from any standard cruise control system.

The time instants of interest in (8) are determined as

$$\begin{bmatrix} t_1 \\ t_2 \\ t_3 \\ t_4 \\ t_5 \end{bmatrix} = \begin{bmatrix} t \\ t-\delta \\ t-\delta^2 \\ t-\delta^3 \\ t-\delta^4 \end{bmatrix}.$$

Here t is a vehicle's estimated link arrival time, $t = t_{n,i_m}^{\text{arr}}$, and δ is the smallest look-back time determined based on the free-flow travel time on the link, as defined in Claes (2015):

$$\delta = \sqrt[4]{\widehat{\tau}_{i_m}^{\text{L,ff}}}. \tag{9}$$

In order to ensure that inputs to the ANN are unique, the size of the discretization time-step $\widetilde{T}$ should satisfy $\widetilde{T} < \delta$.

Note that the inputs: occupancy of the downstream links, and the desired vehicle speed, in (7) are an addition to the neural network inputs employed by Claes (2015). The occupancy of the downstream links helps to predict spillback effects, thus improving the prediction accuracy of congested travel times. The desired vehicle speed captures the stochasticity in individual travel times from heterogeneity in speed preferences, especially improving the prediction of free-flow travel times.

3.4. Artificial neural networks for travel time prediction

Each link agent employs an independent artificial neural network (ANN) to predict time-dependent travel times. We use a fully connected feedforward ANN with 1 input, 1 hidden, and 1 output layer, as shown in Fig. 3. The input layer includes 6 fixed input neurons, and some variable inputs depending on the number of exiting links downstream of the prediction link; a hidden layer using 3 neurons; and an output layer using a single neuron that outputs the scaled travel time prediction. The architecture of the ANN is simple, making it straightforward to train, to analyze, and to prevent overfitting over the training dataset. The ANN weights are trained using the Levenberg–Marquardt modification of the backpropagation algorithm (Hagan and Menhaj, 1994). In this method, the least square error is minimized over a batch of input-output pairs in the training dataset. To optimize for performance accuracy over unseen data-points, it is common to add a regularization term that penalizes high values of the ANN weight parameters. We however do not use regularization, as the inherent stochasticity in simulation-generated training dataset is sufficient to prevent overfitting. The traffic interpretation of the ANN inputs was described in (7). The training efficiency thus achieved for the link predictors in our simulation networks will be discussed in Section 5.3. Note that the influence of varying penetration rates and traffic conditions on the prediction performance of link predictors (for a similar ANN architecture) have been studied in a previous work (Mahajan et al., 2017).

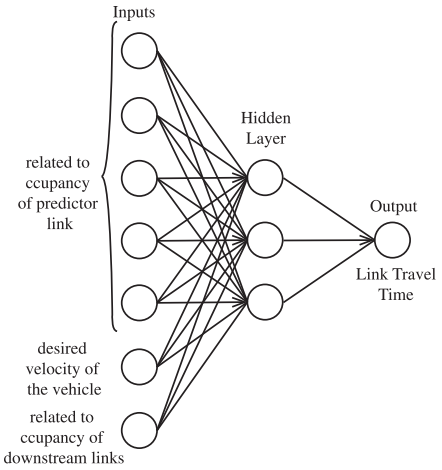

Fig. 3. ANN architecture used by infrastructure agents to predict link travel times.

4. Properties of the routing system

In this section, we discuss the routing system qualitatively, focusing on some properties that result directly from its design. These properties influence the route travel time prediction accuracy, and UE performance, forming a basis for the quantitative analysis presented in Section 5.

4.1. Prediction accuracy depends on route length

In a predictive routing strategy, the routing decisions are determined based on estimates of future travel times on different routes. Thus, the routing performance is subject to the accuracy of the travel time predictions. In the strategy we use, the route travel times are estimated as the sum of the constituent link travel times. It furthermore requires link predictors to cooperate by sharing information with their immediate neighbors. The exchange is similar to that between discrete network elements in macroscopic traffic prediction models, where the output from one network element forms the boundary condition for the subsequent. Link travel times predicted sequentially within such a distributed framework are prone to error propagation. It is expected that a prediction error in an upstream link may influence the prediction accuracy of a further downstream link, such that it results in growing errors in total travel time estimates over multiple links. Understanding the relation between the link travel time prediction errors and the route travel time prediction error will result in design requirements for link predictor accuracy if the desired route prediction accuracy is known (say, as a reliability requirement). Furthermore, the error propagation behavior dictates if the proposed prediction approach is suitable for more complex networks with longer routes, where predictions from many more link-predictors would influence the route travel time estimates. To that end, we investigate error accumulation over multiple links in Section 5.3.

4.2. Control settings

The routing strategy uses two important tuning parameters that influence the controller response to the traffic dynamics: the parameter α in the probabilistic route selection criterion in (1), and the control interval T. The importance of the choice of these parameter values is discussed below.

4.2.1. Stochastic routing parameter

The routing parameter α in (1) determines the sensitivity of the probability of switching routes to travel time gains on a faster alternative. Fig. 4, plotting the route switching probability function for different α-values and percentage improvement in travel time between two alternatives, shows how the choice of the parameter can influence routing dynamics. A higher value of α, for the same relative improvement in travel time, would imply a higher probability of switching to the faster route. In other words, the responsiveness of the routing advice to improvements in travel time is higher for higher values of α. At the same time, a high responsiveness can also result in unstable or oscillating route choice behavior, with high fluctuation in routing decisions from small differences in travel times. For extreme values of the parameter, say $\alpha \geqslant 100$, even a 5% improvement would trigger vehicles to switch routes with near 100% probability. In such a setting, the control behavior will be similar to a bang-bang type controller, wherein vehicles switch to a faster route for any improvement (big or small) in travel time. In contrast, notice in the plot how for values of $\alpha \gtrapprox 5$, only an improvement larger than $\approx$ 50% guarantees that the vehicle would switch to the faster route. In contrast, there are significant differences in response with different α values for lower travel time gains, where the functions tend to behave more linearly.

The role of the parameter α can be compared to the gain constant in a P-type (proportional) predictive feedback controller used in Wang et al. (2003). A subtle difference is that the value of the proportional gain constant directly determines how strongly the splitting-ratios are adjusted for estimated differences in route travel times, whereas α affects the likelihood of a single vehicle agent

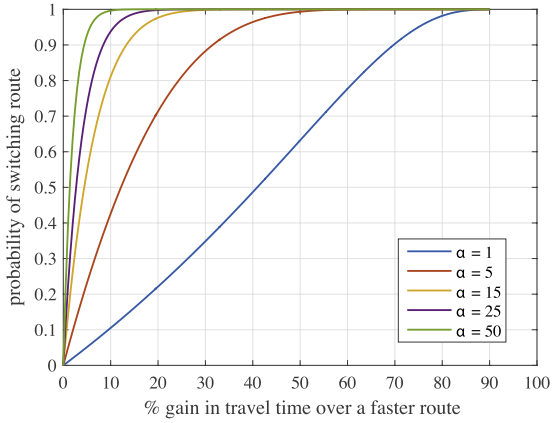

Fig. 4. Influence of route selection parameter on switching probability to a faster route.

re-routing based on the estimated travel time gain.

4.2.2. Control interval

The control interval T determines how often the control decisions are re-evaluated. Choosing a small value of T ensures sufficient iterations for the intentions to converge to an equilibrium solution, fast enough to adapt to (new) disturbances. At the same time, the control interval T is a design variable that directly influences both the communication and computation load of the link agents. With growing network size, the number of vehicles in the network increases, and the number of link agents a vehicle queries in order to receive route travel time estimates also increases. In order to ensure that each vehicle receives travel time predictions over all candidate routes before the next exploration event, a higher control interval may be necessary with increasing network size. Overall, from an infrastructural perspective, the highest possible control interval T that does not deteriorate equilibrium performance is most desirable.

Although, the influence of these parameter choices are now qualitatively understood, their effect on the equilibrium performance (predicted or actual) are unknown. Thus, we study the network equilibrium performance for different values of parameters α and T in Sections 5.4.1 and 5.4.2, respectively.

4.3. Equilibrium mechanism

The control dynamics can be observed at two different levels – one, at the level of an individual vehicle, updating its routing decisions at regular intervals, and two, at the network level, as the resulting traffic behavior from the collection of decisions of all controlled vehicles (upstream of a routing decision point) at a given time instant. Using the two observation levels helps in underpinning how the bottom-up control reaches network equilibrium.

4.3.1. Convergence of vehicle intentions

We define convergence of a vehicle intention as the process of a vehicle's plan stabilizing to the minimum travel time path. However, the quality of the decision a vehicle makes indirectly depends on the quality of decisions of other vehicles in its environment. More specifically, a vehicle's routing decision is influenced by vehicles that arrive at a decision point before it, other vehicles that similarly influence these vehicles, and so on. Let us call them the 'vehicles of influence'. From a vehicle's perspective, if the decisions of the 'vehicles of influence' have already converged to the equilibrium (minimum travel time) plans, the given vehicle can also converge to its optimal route choice. In contrast, if the 'vehicles of influence' keep changing their decisions – due to varying traffic conditions or due to the controller settings – an upstream vehicle may not reach a stable decision before it arrives at a decision node, and thus may commit to a sub-optimal decision. In a multiple OD network, it is also possible that traffic flows between all OD pairs have not converged to their equilibrium route plans.

4.3.2. Convergence of actual travel times

The convergence of the actual travel times depends on the decisions of all IVs upstream of a diverge location. These collective route intentions inform the link predictors of a (possible) future traffic distribution. Using this potential traffic condition, the predictors provide a travel time estimate, which then the vehicles use to update their plans. In repeating this process over multiple control time-steps, the routing system can explore different traffic distributions dynamically. Only once the collective intentions have settled to an equilibrium distribution (under stationary traffic conditions), the resulting network state can settle to an equilibrium.

An exact equilibrium solution requires that the system achieves a steady-state in which travel times over all used routes between an OD pair are equal, and the unused routes have larger travel times. In (Du et al., 2014), the authors have proven the existence of a user equilibrium condition for a similar strategy that uses a multinomial logit route choice model based on expected future traffic conditions (also determined with the latest traffic flow information and route choice proposals of vehicles). The key assumption here is of a continuous and strictly increasing link cost function, which they meet by choosing a BPR function to model link costs. Despite the fact that our approach based on neural networks does not guarantee the same condition, even when a unique equilibrium solution does exist, the system may not be able to exactly reach it in real traffic. This can be expected for the following reasons: (i) the neural network based link predictors have a less than 100% accuracy, as they do not capture all sources of heterogeneity in driving characteristics that lead to travel time stochasticity, (ii) the route choice criterion results in a switching probability $0 \leqslant p < 1$ to choose the fastest available alternative, such that a vehicle has a probability $1 - p$ of accepting the sub-optimal decision of keeping its current route, and (iii) the traffic process is discrete; adding a single vehicle on a route is a discrete change, and the travel time delay caused by this extra vehicle is not a continuous function.

Traffic disturbances often lead to non-stationary traffic states. The routing system may take some time before a (near-) equilibrium condition is reached. Therefore, we study the dynamics of the system towards equilibrium from a perturbed state in Section 5.5.

5. Simulation analysis

In the previous section, we discussed qualitatively some important design aspects for an effective implementation of the routing system. In this section, we will use a simulation-based evaluation to study quantitatively: the influence of the link predictors' design on prediction accuracy, the impact of the control settings on system performance, and the traffic dynamics in reaching equilibrium. To that end, we first explain the set-up of the simulation experiments, the criteria used for evaluation, and subsequently discuss the

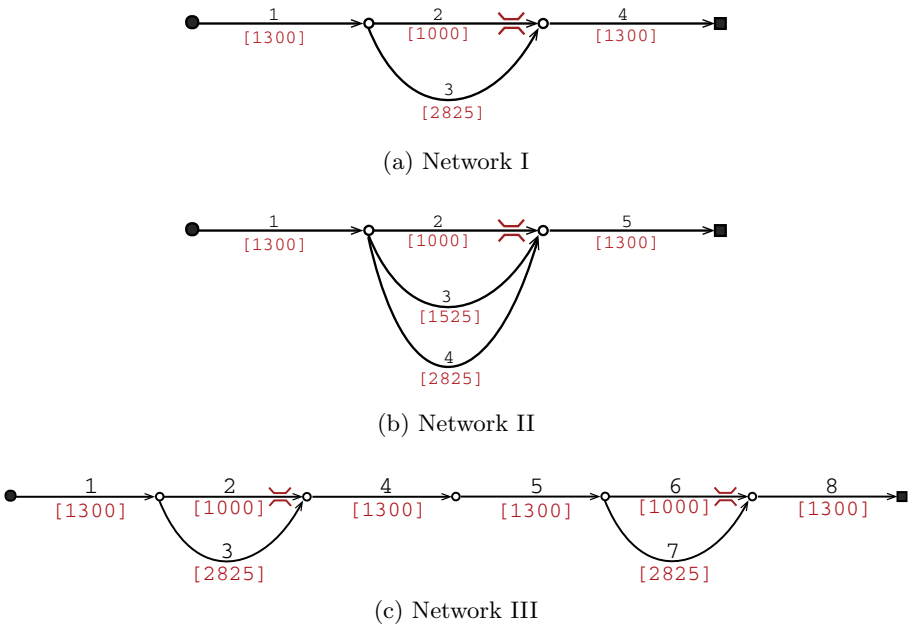

Fig. 5. Test networks with link index indicated above (black) and the link length in meters below (red). The red symbol on links 2 and 6 indicate a lane-drop bottleneck. (For interpretation of the references to colour in this figure legend, the reader is referred to the web version of this article.)

results obtained. The evaluation is conducted using the VISSIM micro-simulation tool. The simulator models stochastic traffic behavior using a distribution for desired speed of vehicles, different driver parameters, and a random arrival process.

5.1. Traffic networks and demand scenarios

Three test networks are modeled, as shown in Fig. 5, which are examined for the demand profiles shown in Fig. 6. Network I is a 2-lane bypass network between a single OD pair. The shorter link has a lane-drop bottleneck, and the longer bypass link has adequate capacity, such that the link stays in free-flow condition even when a high traffic volume is diverted towards it.

In Network II, the network complexity is increased by using an additional route alternative. The network has two 2-lane bypass links of different lengths. The shorter bypass link has a road gradient (uphill slope) of 18%; the deceleration behavior due to the slope can trigger congestion as the link flow increases. Thus, the bottleneck limits the capacity on the shorter bypass link, making the longer bypass favorable in high demand situations. This network setup allows to test the stability of the routing response: if convergence behavior exhibits oscillations between the route alternatives. Finally, Network III replicates Network I twice. This network doubles the number of route alternatives, and also increases the length of each alternative compared to the other networks. Table 1

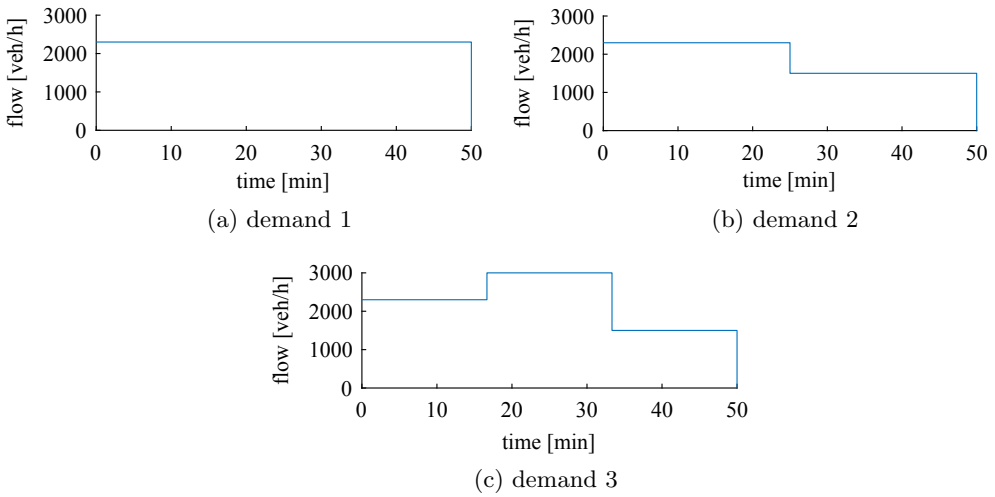

Fig. 6. Different demand profiles used in simulation.

Table 1
Route properties.

	Route	Route topology	Total length [km]	Free-flow travel time [min]
Network I	1	1–2–4	3.600	2.9
	2	1–3–4	5.425	4.0
Network II	1	1–2–5	3.600	2.9
	2	1–3–5	4.125	3.3
	3	1–4–5	5.425	4.0
Network III	1	1–2–4–5-6–8	7.200	4.9
	2	1–2–4–5–7–8	9.025	6.0
	3	1–3–4–5–6–8	9.025	6.0
	4	1–3-4–5–7–8	10.850	7.1

provides the properties of each route in the test networks. We can further work out that in Network I and II, the free-flow travel time on the longest route (route 2 and route 3, respectively) is roughly 38% higher than the shortest route (route 1), and in Network III the difference is roughly 45%.

5.2. Equilibrium performance criteria

In Section 4.3, we discussed that due to properties of traffic and the control system, an exact equilibrium solution may not be reached. In order to quantify the extent of disequilibrium, we define an *a posteriori* criterion that can be used to compare the performance in cases with different parameter settings, for a given network structure and demand pattern. The loss function L gives the average excess travel time that a vehicle experiences from not taking the minimum cost route:

$$L = \frac{\sum_{n\in N} \left(\tau^{\mathrm{R}}_{n,r}(t^{\mathrm{arr}}_{n,i_1}) - \tau^{\mathrm{R}}_{n,r^*}(t^{\mathrm{arr}}_{n,i_1})\right)}{|N|}. \tag{10}$$

In the above formulation, the travel time loss for each vehicle is determined by comparing the actual travel time $\tau^{\mathrm{R}}_{n,r}$ it spends in the network, to the travel time on the fastest alternative r^* at the time that the vehicle entered the network. Note that the numerator in the above expression is always non-negative. The set N includes vehicles that enter the network while the predicted travel times are in equilibrium; $|N|$ denotes the cardinality (number of elements) of the set. The equilibrium condition is detected using a tolerance ζ for the relative difference in predicted route travel times compared to the fastest route; we use $\zeta = 0.01$ in our simulations.

An expression similar to (10) can be formulated using predicted route travel times. We denote the average predicted loss in disequilibrium as $\hat{L}$. In this criterion, the numerator gives the aggregated difference between the predicted travel time on the chosen route and the predicted fastest route for all vehicles in set N. The predicted loss $\hat{L}$ is a result of the stochastic decision-making, due to which a vehicle may take a route other than the predicted fastest route. Thus, if the route travel time predictions are accurate, then $\hat{L}$ expresses the ideal performance of the routing system. The performance difference between the predicted loss $\hat{L}$ and the actual loss L relates to the inaccuracy of the route travel time predictions.

5.3. Error propagation along link travel time predictors

We first discuss the accuracy of ANN-based link predictors, and then analyze the error propagation between predictors. Table 2 summarizes the accuracy of all link agents in the test networks. In all networks, the bottleneck links perform worse compared to the other links that do not get congested. This is expected, as the ANN does not explicitly model queuing behavior, and the inputs may be too simple for capturing congestion dynamics. In both the cases of lane-drop and gradient bottlenecks, infrastructural properties of the link trigger congestion and influence the congestion dynamics. Thus, inputs related to infrastructural properties and congested traffic state could be used to further improve the accuracy of the link predictors.

In order to investigate a potential accumulation of prediction errors over routes with multiple links, we use relative cumulative error ϵ, given as

Table 2
Prediction performance of the link predictors in the test networks.

		Percentage absolute relative errors [%]							
Link number		1	2	3	4	5	6	7	8
Network I	train	3.83	7.36	2.45	3.07	–	–	–	–
	Test	4.10	7.04	2.49	3.07	–	–	–	–
Network II	train	3.90	10.17	3.10	17.58	3.50	-	-	-
	test	3.92	10.17	2.84	17.20	3.36	–	–	–
Network III	train	3.65	9.03	2.14	3.63	4.12	7.08	2.24	3.38
	test	3.65	8.94	1.99	3.65	4.29	6.89	2.22	3.46

$$\epsilon = \frac{\sum_{j\in S}(\tau_j^L - \hat{\tau}_j^L)}{\sum_{j\in S}\tau_j^L}, \tag{11}$$

where the numerator is the total absolute error for a combination of links $S \subseteq I_r$, where sequence $I_r = (i_1, i_2, \ldots, i_M)$ includes the links along route r; the denominator is the corresponding total actual travel time for links in S. Let ϵ_j be the relative error on a given link,

$$\epsilon_j = \frac{\tau_j^L - \hat{\tau}_j^L}{\tau_j^L}. \tag{12}$$

Then, we can rewrite (11) in terms of relative link errors as

$$\epsilon = \frac{\sum_{j\in S}(\epsilon_j\ \tau_j^L)}{\sum_{j\in S}\tau_j^L}. \tag{13}$$

If the individual link travel times are assumed to be constant (time invariant), then the above formulation becomes a weighted sum of the individual relative link errors

$$\epsilon = \sum_{j\in S}(w_j\ \epsilon_j), \tag{14}$$

$$w_j = \frac{\tau_j^L}{\sum_{j\in S}\tau_j^L},$$
$$\sum_{j\in S} w_j = 1.$$

If we also assume link errors to be distributed independently, the variance in relative cumulative error ϵ can now be given as

$$\mathrm{Var}(\epsilon) = \sum_{j\in S}(w_j{}^2\mathrm{Var}(\epsilon_j)). \tag{15}$$

Thus, we can conclude that with time invariant link travel times and independently distributed link errors, the variance in route error will always be less than the maximum variance in relative link errors:

$$\mathrm{Var}(\epsilon) < \max_{j\in S}(\mathrm{Var}(\epsilon_j)). \tag{16}$$

In order to verify the above conjecture, we use simulation data for a scenario with a constant demand of 2200 veh/h and a splitting ratio of 0.85 towards route 1 in Network III. We use this data to first evaluate the statistical correlation between link errors. The Pearson correlation coefficients – indicative of a linear correlation between relative errors on any two links – are provided in Table 3. The link errors show a weak correlation, given that the significant correlation values range between -0.05 and 0.11. Even so, link travel times and hence the weights in (14) are not constant (refer to Table 4), as is expected in real traffic as well. Therefore, the theoretical finding in (16) may not hold in practice.

On further analysis, we find that the maximum variance in relative link errors ϵ_j is 0.403 for link 8 (refer to Table 3). The mean and variance in relative route errors ϵ are -0.034 and 0.004, respectively. We note that the error variance for the route (0.004) is not just significantly less than the maximum variance in link errors (0.403), it is even less than the minimum variance in link errors (0.005 for link 4). In Fig. 7, we plot the probability distribution of errors ϵ for combination of links, starting with the most erroneous link predictor and consecutively adding links in decreasing order (link 8, 2, 1, 6, 5, and 4) of the variance in relative link errors. We observe that the spread of the probability distribution curves reduces as the link predictions are aggregated. The result is relevant from a design perspective – if link predictors of pre-defined accuracy are used, then the route travel time predictions can be expected to be not less accurate than the least accurate link. This also means that for desired prediction accuracy at the route-level, link predictors of at least the same accuracy must be employed.

Table 3
Pearson correlation coefficients, mean, and variance for relative travel time errors on links along route 1 in Network III.

	Correlation*						Mean	Var
Link number	1	2	4	5	6	8		
1	–						−0.037	0.032
2	**−0.044**	–					0.001	0.377
4	−0.006	**−0.019**	–				−0.001	0.005
5	**0.030**	**−0.026**	**0.107**	–			−0.003	0.011
6	−0.007	**0.069**	−0.003	**0.025**	–		0.040	0.015
8	−0.003	**−0.026**	0.010	0.010	**0.061**	–	−0.057	0.403

* Significant correlation values ($p < 0.05$) are highlighted in bold.

Table 4
Mean and standard deviation for the weights in Eq. (14) for links on route 1 in Network III.

Link number	1	2	4	5	6	8
Mean	0.096	0.330	0.162	0.192	0.184	0.229
SD	0.045	0.152	0.052	0.073	0.093	0.113

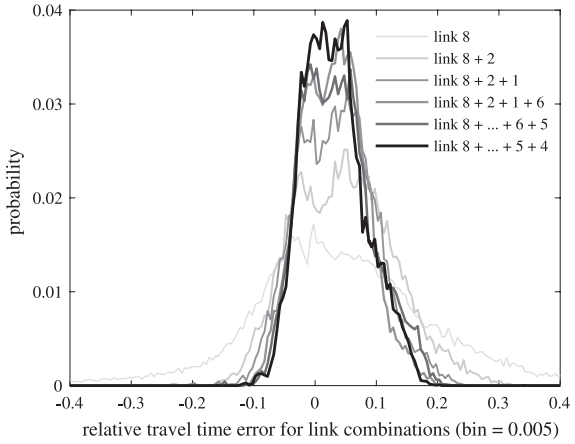

Fig. 7. Histogram plot-shape for relative cumulative error over links on route 1 in Network III.

5.4. Influence of control parameters

5.4.1. Stochastic routing parameter

In this sub-section, we examine the effect of parameter α on control stability and equilibrium performance. The simulation experiments use demand profile 1, and different values of α = 1, 5, 15, 25, 35, 45 and 50. We first look at how the route plans of individual vehicles (independent controllers) evolve over time. The convergence of individual vehicle plans implies control stability, which means that the vehicles' routing decisions do not keep oscillating between the route alternatives but instead stabilize over time. In an ideal control scenario, for an optimal equilibrium solution, each vehicle should converge to a stable routing plan before arriving at a bifurcation node.

Fig. 8 compares, for different values of α, the temporal dynamics of the total number of switches in individual route plans upstream of the first bifurcation node. The figure shows results for Network I with demand profile 1 and control interval T = 1. Similar results were observed for increasing values of α in the other networks. The results show that increasing α increases the

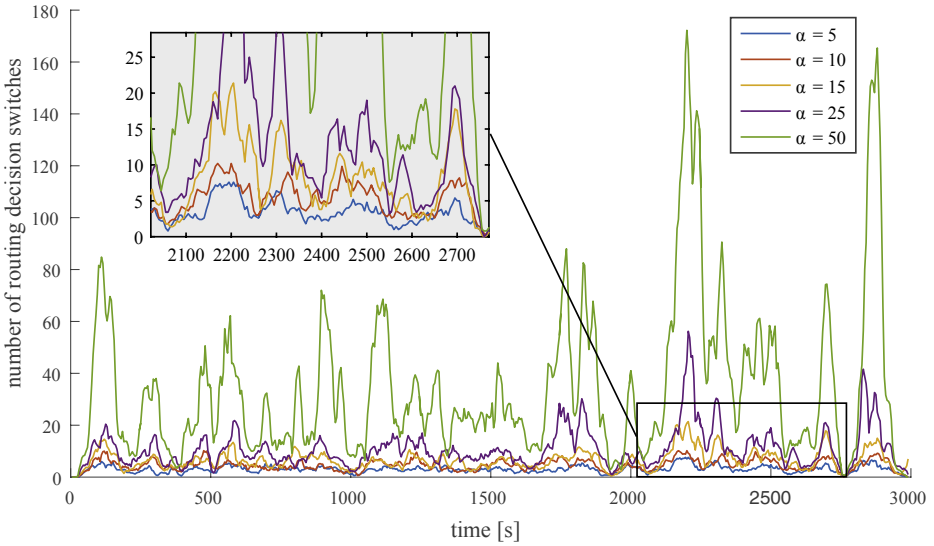

Fig. 8. Influence of route selection parameter on controller stability.

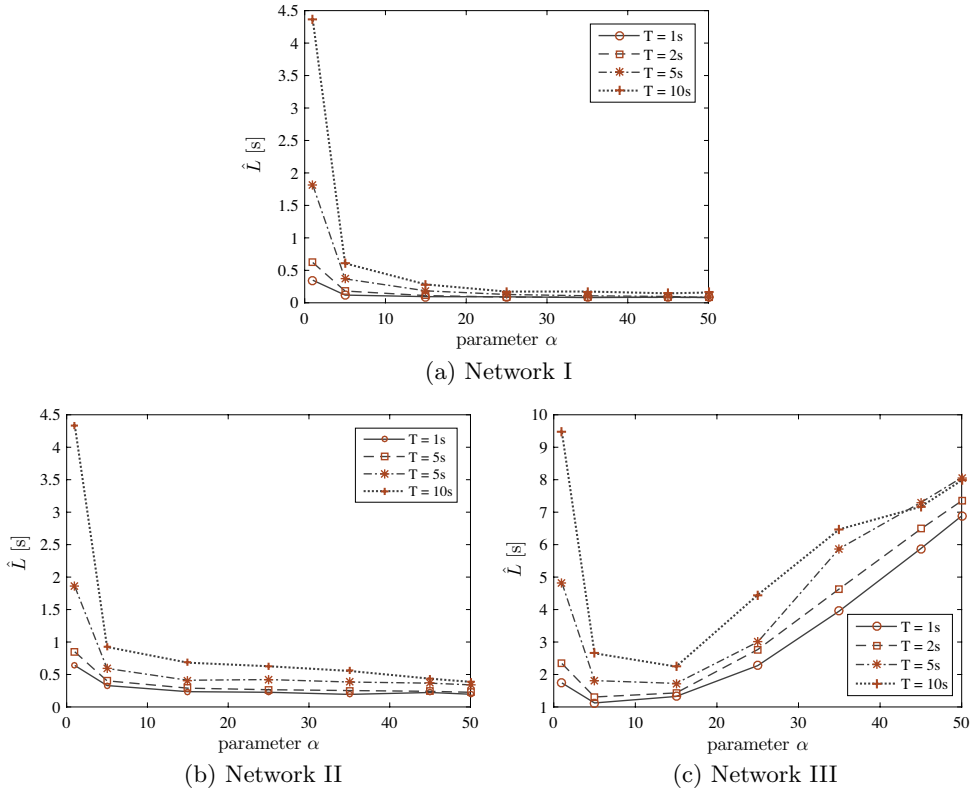

Fig. 9. Predicted travel time loss in disequilibrium per vehicle for different parameter values.

fluctuations in the total number of switches over time. These fluctuations may continue to intensify, as is best observed in the switching dynamics for $\alpha = 50$. However, internally fluctuating routing decisions do not necessarily imply unstable network dynamics. The route travel times can still be converging towards equilibrium. Only when fluctuations in decisions result in traffic dynamics that oscillate about the equilibrium point and the magnitude of the overshoot (in either direction) increases over time, the controller becomes unstable.

To further investigate if there is a trade-off between stability gain and network performance, we compare the disequilibrium loss in predicted travel times $\hat{L}$ and actual travel time L for the different control settings. Since the estimated travel time loss $\hat{L}$ excludes the influence of prediction inaccuracies, any differences in $\hat{L}$ values are a direct measure of the influence of the control parameter values on the equilibrium dynamics. Fig. 9 illustrates the impact of α on the loss function $\hat{L}$ in the three networks. A consistent result in all the networks is that an extremely low value of $\alpha = 1$ results in slow control response, significantly deteriorating equilibrium performance. However, the results suggest that the overall equilibrium performance does not degrade even for very high values of α in Networks I and II. This could be due to fewer route alternatives in these networks, such that the increasing internal fluctuations in routing decisions result in a random route choice which is better for the equilibrium performance. Additionally, the loss function curve tends to flatten beyond $\alpha = 25$, which supports the reasoning that in simple networks, it is the randomness from the oscillations that influences performance, and the intensity of the oscillations per se becomes irrelevant.

In contrast, the results for Network III in Fig. 9c are more in line with our expectation for real networks. We see that if α is too small, the control response is too slow to equilibrate travel times over multiple routes. When α is too big, the control response is stronger than necessary and the fluctuations in control decisions deteriorate predicted equilibrium performance. The optimal choice of α for Network III is then 5 or 15, depending on the control interval. We will discuss the relation between α and T in the following section.

Table 5 summarizes the actual travel time loss in disequilibrium per vehicle L for different control settings. Unlike the results for average predicted loss in Fig. 9, the variation of L with parameter α is less regular in all three networks. This is perhaps because the error of the travel time predictors dominate the actual equilibrium performance, which are of the same order. The value of L for Network I ranges between 8–13 s, which is roughly 5–8% of the free-flow travel on the shortest route in the network; the link predictor errors in Network I also lie in a similar range (Table 2). The actual disequilibrium loss in Network II and III ranges between 17–22 s per vehicle, which is roughly 10–13% and 6–8%, respectively, of the free flow travel time on their shortest routes.

5.4.2. Control interval

By varying the control interval T in different networks, we investigate if a threshold value of T can be found, that balances the trade-off between equilibrium performance and communication and computation load. We also discuss how the choice of T relates to

Table 5
Actual travel time loss in disequilibrium per vehicle [s] for different parameter values; the lowest loss values are marked with a *.

	Network I	Network II	Network III	Network I	Network II	Network III
α		$T = 1s$			$T = 5s$	
1	8.66*	19.09	18.41	10.38	21.36	18.28
5	9.74	19.85	17.97	8.92	19.01	17.35
15	8.73	19.34	17.54	8.74	19.30	18.40
25	9.20	20.24	19.10	8.87	19.41	18.17
35	9.26	20.63	16.97	9.23	19.16	16.30*
45	8.67	19.97	16.72*	9.10	19.45	17.38
50	8.85	17.97*	17.48	8.71*	17.73*	16.46
α		$T = 2s$			$T = 10$ s	
1	9.03	19.44	17.68	12.74	22.43	21.02
5	8.34	19.45	18.09	9.17	19.64	18.44
15	9.07	19.06	17.83	8.49	19.72	17.46
25	10.23	18.77	17.50	8.95	18.93	17.08
35	8.26*	19.67	17.95	8.70	18.81	17.59
45	9.30	19.85	18.08	8.37	18.80	16.93
50	8.26*	17.75*	16.62*	8.00*	17.86*	15.78*

the value of α, and identify the optimal control settings in the test networks.

The results in Fig. 9 are also relevant here. In all test networks, increasing the value of T shifts the trend line slightly higher, indicating a loss in equilibrium performance. However, the performance loss is marginal for higher values of α, especially in Networks I and II. This implies that for networks with fewer route alternatives, a larger control interval is advantageous. Furthermore, in Fig. 9c, an important relation between α and T is evident. Notice that for lower values of $T = 1$ and 2, the optimal value of α is 5, however, for higher values of $T = 5$ and 10, $\alpha = 15$ is preferable. This is justified because, a larger T means fewer iterations for convergence and thus a slower equilibrium response. Then a stronger responsiveness from a higher value of α can be compensating. Therefore, when practical limitations necessitate a higher T, a higher value of α is desirable, or in other words, a smaller α in general requires a smaller T.

We can now identify the most suitable parameter settings in the three networks. Since choosing a higher T is useful for scalability, and since the predicted loss $\widehat{L}$ is only slightly higher compared to lower T values, we choose $T = 10$ s in Network I and $T = 5$ s in Networks II and III. For these optimal T values, we look for the largest α that does not deteriorate network performance. We choose an $\alpha = 25$ for Network 1 and $\alpha = 15$ in Networks II and III. The α values in Networks I and II are conservative, but they ensure control stability with only a slight increase in disequilibrium loss. In Section 5.5, we will use these parameter settings to analyze the equilibrium dynamics in the test networks.

5.4.3. Tuning control parameters in practice

In the above analysis, we find that even in our simple test networks with 1 OD pair, the desirable values for the control parameters depend on the network structure. Moreover, the choice of the routing parameter and the control interval is found to be interdependent. Thus, in order to implement the routing system in a real network, a tuning procedure would be required to identify the optimal parameter setting. Based on our simulation results, we recommend an online tuning procedure as such:

1. Choose a minimum control interval T based on the available communication bandwidth, such that the vehicle and link agents can interact reliably, i.e. vehicle agents can complete one cycle of intention propagation, exploration and decision update within the duration T.
2. Gradually increment the value of the routing parameter α between 5 and 50, until the maximum value of α that still results in a reduction of the disequilibrium loss (defined as the excess travel time a vehicle incurs on a non-minimum cost route) in predicted route travel times is found.
3. If T can still be increased given its initial choice, gradually increase T in steps of <5 s to find the maximum value for which the routing performance remains within policy dictated efficiency limits.

5.5. Dynamics towards equilibrium

This sub-section investigates how the predicted and experienced travel times evolve, the splitting-ratio achieved from the routing approach, and the resulting quality of convergence. The travel time a vehicle predicts upon entering the network depends on the collection of decisions of all vehicles between the network input and a decision node at the time of prediction, while the experienced travel time depends on the vehicle's final plan before they cross the decision node. Thus the difference between the two results from the convergence of collective plans during the time it takes the vehicle to reach the decision node. Given the control settings and demand pattern, the convergence behavior determines the realized quality of equilibrium. We define quality of equilibrium as the maximum relative travel time difference between any two used routes, over a given horizon from the time that a near-equilibrium

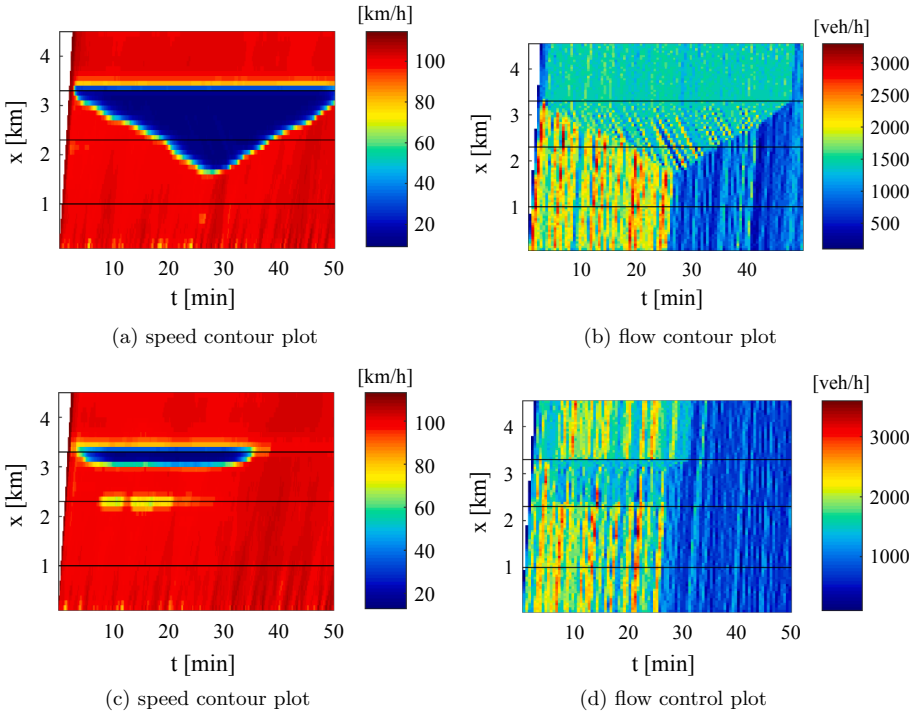

(a) speed contour plot (b) flow contour plot

(c) speed contour plot (d) flow control plot

Fig. 10. Dynamics on the shortest route 1 in Network I using demand 2. Subfigures (a) and (b) show the no control case (TTS = 153.4 veh.h), and (c) and (d) the controlled case (TTS = 76.6 veh.h).

state is detected.

To first understand the response of the routing controller from a traffic flow perspective, Fig. 10 plots the speed and flow contour plots for route 1 in Network I with and without the routing strategy in use. We use demand profile 2 for these examples, so as to ensure that the congestion does not spill back to the start of the network in the no control case. For the no control case, we assume naive routing, that is all vehicles choose the shortest route without considering the traffic condition on the routes. In the control case, the routing strategy is active from the start. Notice in Fig. 10c and d that a short queue is stably maintained at the bottleneck as both routes are used in equilibrium. Thus, utilizing the bypass route when the demand is high prevents congestion spillback. Furthermore, the network outflow is higher in the control case, resulting in a roughly 100% gain in total time spent (TTS). The outflow increases because the flow on link 5 is the total of the queue discharge from the bottleneck and the rerouted flow from the bypass. Once the demand reduces, the equilibrium state uses only the bottleneck route, resulting in the same outflow as in the no control case.

We analyze the traffic dynamics with route guidance using the step demand 3 in Fig. 6c. The results for the test networks are shown in three sub-plots. The first two sub-plots show the relative differences in predicted and actual travel times, as a ratio between 0 and 1, wherein each curve indicates the relative difference between the travel time on a route and the lowest travel time in the network at a given time. The third sub-plot provides the splitting-ratio at the most upstream diverge node in the network. Notice in Fig. 11a that the first vehicle that enters the network predicts the bypass route to be about 42% slower than the bottleneck route. This difference starts to reduce as the bottleneck route saturates, and controller equilibrates the demand with a splitting-ratio of roughly 0.75 towards route 1, while the inflow is 2300 veh/h. Subsequently, as the demand increases to 3000 veh/s, more vehicles anticipate the bottleneck route to be slower. The result is that the spitting-ratio towards route 1 decreases to roughly 0.55 during the peak. This continues until the inflow drops to 1000 veh/h and all vehicles can take route 1 without activating the bottleneck. Observe that in this period, the predicted relative difference of route 2 (compared to route 1) increases, tending to their relative travel time difference in free-flow condition. Furthermore, the plot for actual relative differences shows the quality of the equilibrium achieved, which is ≈ 13% in Network I.

The results for Network II show that even with more number of alternatives, the routing decisions on average do not oscillate between the two bypass routes. This is evident from the dynamics of the splitting-ratio. As the traffic volume increases, the longest alternative (route 3) carries more traffic volume, from less than 5–20% of the total volume, in order to maintain equilibrium. The maximum relative difference in actual route travel times is about 21% in Network I. The equilibrium quality is thus worse than for Network I. One reason for this is the increase in network complexity, in terms of the number of alternatives. The other reason is the difference in the prediction accuracy of the link predictors in these networks. See in Table 2 that the link predictor on link 3 in Network II has a lower performance than any other link in Network I.

In Network III we see that route 3 is initially preferred to route 2. So even though the routes are equal in length, they are utilized differently. This is due to the difference in bottleneck location on these routes. The routing strategy can predict the resulting

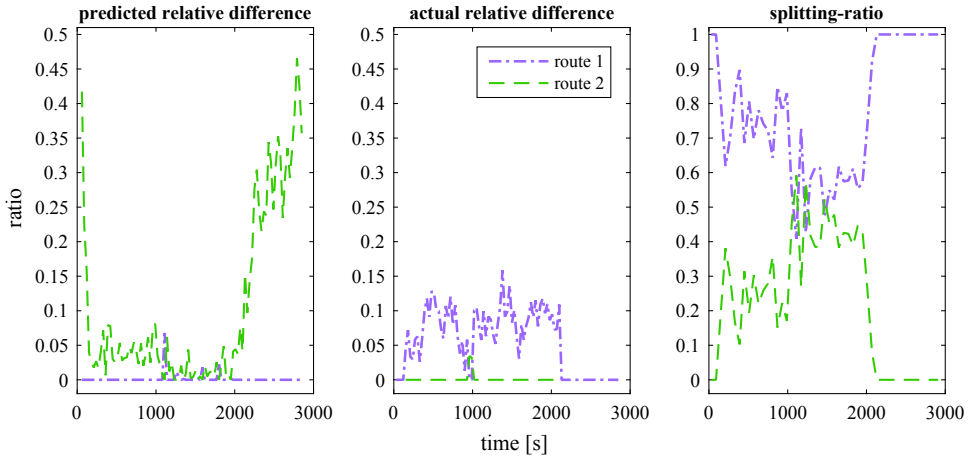

(a) Network I (parameters $\alpha = 25$ and $T = 10\ s$)

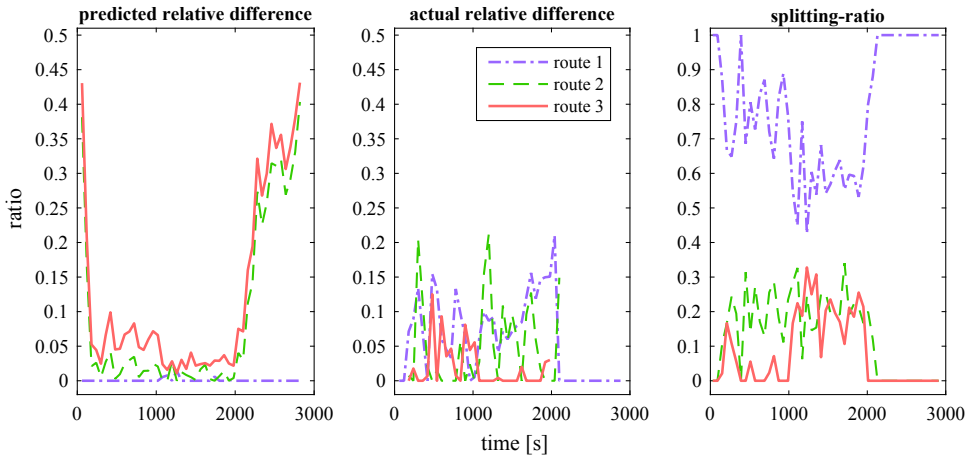

(b) Network II (parameters $\alpha = 15$ and $T = 5\ s$)

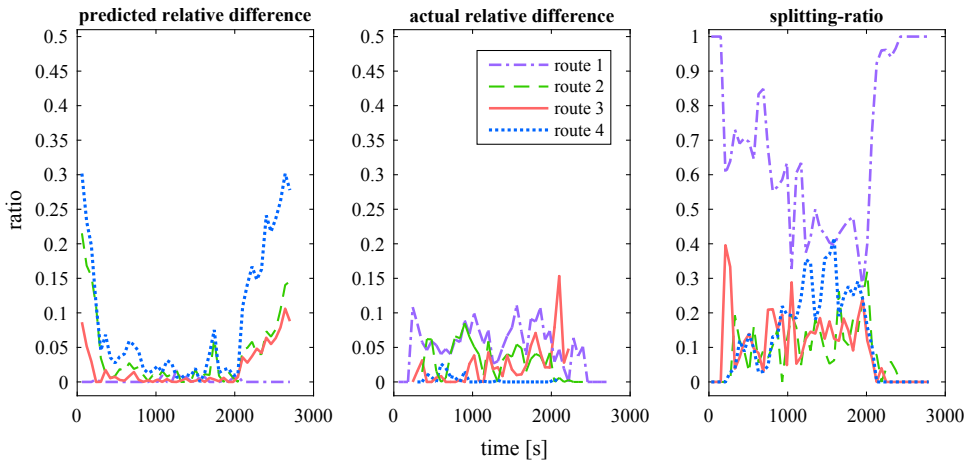

(c) Network III (parameters $\alpha = 15$ and $T = 5\ s$)

Fig. 11. Equilibrium dynamics in the test networks with demand profile 3; relative differences compare instantaneous travel times on a given route with the predicted or actual fastest route at that time.

differences in traffic states and travel times. Once the second bottleneck is triggered, route 4 receives a slightly higher split-fraction compared to the relatively shorter but congested routes 2 and 3. The equilibrium quality thus achieved is about 15 %, which is better than the performance in Network II. This result suggests that even though network complexity influences overall performance, travel time prediction (in) accuracy can dominate its effect.

5.6. Scalability aspects

Scalability can be defined as the property of a control system to perform desirably – given the available infrastructural resources – when scaled to larger networks. In that sense, the scalability of the routing system depends on how the computation and communication requirements grow with network size. The computation requirements in the routing system include: each vehicle agent evaluating its routing decisions (using (1)) once every control interval, and each link agent making predictions based on a (potentially pre-trained) neural network for vehicles in the network considering using the link. While a vehicle agent's computational load remains constant regardless of the network size, for a link agent it increases with the number of vehicles seeking predictions. The increase is however bounded, because trip lengths do not grow indefinitely with network size.

The limiting factor in the routing approach is the communication bandwidth required for vehicles to explore routes and propagate their routing intentions. The communication load grows with the number of vehicles in the network. Similar to the growth of computation load, limited trip lengths mean that the number of communications per exploration or intention propagation event has an upper bound. Moreover, the number of routes that a vehicle explores does not scale indefinitely. Behavioral research suggests that individuals consider a small number of alternatives (about 5) when making routing decisions; and the size of the 'consideration choice set' required for modeling purposes is typically in the same order of magnitude (Bovy, 2009). So the maximum number of exploration agents a vehicle deploys is independent of how the number of routes in a network increases with its size.

Notably, the choice of the control interval T is important with growing network size. A feasible value of this parameter should ensure that even with the maximum latency (highest for vehicles furthest away from a given link agent), vehicles are able to explore routes of different lengths and confirm their updated intentions within the chosen interval. The strategy would fail to scale only when the desirable value of T is too large for timely routing response.

A single vehicle exploration or intention propagation event requires a maximum of $|I_r| + 1$ hops (where $|I_r|$ is the total number of links on a route r); a vehicle agent exploring the complete route takes $|I_r|$ hops between the consecutive link agents on the route, and 1 additional hop to return the route travel time to the vehicle agent. As an example, consider a (conservative) latency of 0.1 s for the communication infrastructure. Then, for a control design using link agents every 1 km, and a control interval of 5 s, a vehicle intention can be propagated within the control interval for trip distances up to 49 km. Furthermore, newer 5G communication technologies are expected to offer much lower latency of 2–5 ms (Hossain and Hasan, 2015), which will increase the feasible network size by a factor of 20–50. We therefore expect all link agents to be able to maintain vehicle intentions consistently, and make real-time predictions based on the latest routing decisions even in large networks.

6. Conclusions and future work

In this work, we have evaluated an integrated travel time prediction and routing algorithm that uses vehicle-level information for generating in-vehicle equilibrium routing advice. The strategy uses the computation and communication potential of intelligent vehicles and artificial neural networks to achieve a decentralized prediction and control structure. Unlike optimization-based predictive approaches, the approach uses reactive decision-making to update individual vehicle routes based on travel time predictions. In this paper, we have analyzed important design aspects that determine the dynamics of the control system and its resulting performance.

We first investigated the artificial neural network (ANN)-based prediction framework. In general, decentralizing the travel time prediction task among multiple link predictors makes the framework independent of network complexity (in terms of the number of OD pairs, number of routes and their lengths). We showed both empirically and theoretically that the accuracy of route travel time predictions is bounded by the accuracy of the least accurate link predictor on that route. The result helps to specify a design criterion for link predictor accuracy, as we now know that the route prediction errors will always be equal to or less than the individual link errors, for any network size. Moreover, it implies that given a minimum accuracy criterion for the link predictors, the route travel time predictions would be more reliable in bigger networks.

Next, we demonstrated a tuning procedure for the control parameters, namely the route selection parameter α and the control interval T. The proposed method is based on minimizing the average disequilibrium loss, defined as the average excess travel time a vehicle may incur from taking a non-minimum cost route. We furthermore found that the disequilibrium criterion based on the predicted travel times, as compared to actual measurements, is more effective for the tuning process. This is because the actual travel times, in addition to the control settings, also depend on the accuracy of the predictions (and of the control decisions based on it). The tuning results show that the choice of the control parameters depends on the network structure. Thus, in Section 5.4.3 we generalized how the control settings could be determined in a real traffic network.

Our analysis furthermore showed the effect of the route selection parameter α on control system stability. Increasing its value increased the fluctuations in individual routing decisions, such that in the largest test network, equilibrium performance improved with increasing value of α only until an optimal value. Beyond this optimal value, the oscillations induced instability lead to increased disequilibrium losses. Thus, we've highlighted how tuning of the parameter α is also linked to its impact on the internal stability of the system.

Through our simulations we were also able to emphasize on the two mechanisms of equilibrium in our system: the internal process wherein the predicted travel times converge, and the external process wherein the actual travel times converge. Comparing the dynamics in predicted and actual travel times over the network routes, we found that the predicted travel times converged much better than the actual travel times. We attribute this difference to the (in) accuracy of the prediction model, which other than the dynamics of the prediction process itself, depends on the training quality of the ANNs.

Training unbiased ANNs can be challenging in practice. We recommend that for (online or offline) training of accurate ANNs, the training dataset must be representative in two ways. One, the examples under saturated traffic conditions should be proportional to the actual occurrence of congestion on the link, and two, the examples should represent the range of link flows observable due to different flow distributions over routes between different OD pairs. Furthermore, we expect that retraining ANNs with a training dataset supplemented with controlled traffic situations can improve prediction accuracy. The accuracy gains achievable from such repeated retraining is relevant from a practical standpoint, and is a question for future research.

There are further possibilities for improvements to the routing system design. For instance, the link predictors could include inputs that capture the influence of infrastructural properties (like gradient, lane-drops, on-ramps etcetera) on the link dynamics, in order to improve prediction performance for complex road layouts. The goal would be to identify the individual vehicle or derived aggregated measurements that are not over-specific, so that a generalized ANN architecture can be used for all links in a network. It would also be interesting to adapt the strategy for asynchronous vehicle explorations and intention propagation. An asynchronous update process implies that the link agents would receive vehicle intentions that were last updated at different time instants in the past. So when a given vehicle updates its intention next, link agents would have to update the specific intention in its record. The link agents must therefore maintain vehicles' identification next to their intentions. Although such asynchronicity is appealing for practice (as it distributes the communication and computation load), it can influence both the accuracy of the link predictors as well as the traffic dynamics in reaching an equilibrium condition. Similar to our work, these impacts can be studied in simulation.

Lastly, the extension of the decentralized routing framework for system optimal routing is an valuable research direction. The estimation of marginal costs for individual vehicles within the decentralized framework is challenging, as it pertains to (also indirect) network effects, which are best estimated in a centralized way. At the same time, decentralized optimization of overall network performance holds the fullest potential of intelligent vehicle technologies. In a methodology similar to ours, Du et al. (2015) show how information perturbation can be used to steer towards system optimality within a distributed framework.

Acknowledgments

The authors would like to acknowledge Technolution B.V. for funding the research in this paper, under the "Spookfiles A58 – Phase 2" project.

References

Adler, J.L., Satapathy, G., Manikonda, V., Bowles, B., Blue, V.J., 2005. A multi-agent approach to cooperative traffic management and route guidance. Transport. Res. B: Methodol. 39 (4), 297–318.
Ben-Akiva, M., De Palma, A., Isam, K., 1991. Dynamic network models and driver information systems. Transport. Res. A: Gener. 25 (5), 251–266.
Bovy, P.H.L., 2009. On modelling route choice sets in transportation networks: a synthesis. Transp. Rev. 29 (1), 43–68.
Claes, R., 2015. Anticipatory Vehicle Routing. PhD thesis. Katholieke Universiteit Leuven, Belgium.
Claes, R., Holvoet, T., Weyns, D., 2011. A decentralized approach for anticipatory vehicle routing using delegate multiagent systems. IEEE Trans. Intell. Transp. Syst. 12 (2), 364–373.
Cong, Z., De Schutter, B., Babuška, R., 2013. Ant colony routing algorithm for freeway networks. Transport. Res. C: Emerg. Technol. 37, 1–19.
Diakaki, C., Papageorgiou, M., Papamichail, I., Nikolos, I., 2015. Overview and analysis of vehicle automation and communication systems from a motorway traffic management perspective. Transport. Res. A: Pol. Pract. 75, 147–165.
Du, L., Han, L., Chen, S., 2015. Coordinated online in-vehicle routing balancing user optimality and system optimality through information perturbation. Transport. Res. B: Methodol. 79, 121–133.
Du, L., Han, L., Li, X.-Y., 2014. Distributed coordinated in-vehicle online routing using mixed-strategy congestion game. Transport. Res. B: Methodol. 67, 1–17.
Garcia, A., Reaume, D., Smith, R.L., 2000. Fictitious play for finding system optimal routings in dynamic traffic networks. Transport. Res. B: Methodol. 34 (2), 147–156.
Grzybek, A., Danoy, G., Bouvry, P., Seredynski, M., 2015. Mitigating flash crowd effect using connected vehicle technology. Veh. Commun. 2 (4), 238–250.
Hagan, M.T., Menhaj, M.B., 1994. Training feedforward networks with the Marquardt algorithm. IEEE Trans. Neural Netw. 5 (6), 989–993.
Hajiahmadi, M., Knoop, V.L., De Schutter, B., Hellendoorn, H., 2013. Optimal dynamic route guidance: a model predictive approach using the macroscopic fundamental diagram. In: 16th International IEEE Conference on Intelligent Transportation Systems-(ITSC), pp. 1022–1028.
Hegyi, A., De Schutter, B., Hellendoorn, H., 2005a. Model predictive control for optimal coordination of ramp metering and variable speed limits. Transport. Res. C: Emerg. Technol. 13 (3), 185–209.
Hegyi, A., De Schutter, B., Hellendoorn, J., 2005b. Optimal coordination of variable speed limits to suppress shock waves. IEEE Trans. Intell. Transport. Syst. 6 (1), 102–112.
Helbing, D., Schönhof, M., Stark, H.U., Holyst, J.A., 2005. How individuals learn to take turns: emergence of alternating cooperation in a congestion game and the prisoner's dilemma. Adv. Complex Syst. 8 (01), 87–116.
Hossain, E., Hasan, M., 2015. 5g cellular: key enabling technologies and research challenges. IEEE Instrument. Measur. Mag. 18 (3), 11–21.
Jennings, N.R., Sycara, K., Wooldridge, M., 1998. A roadmap of agent research and development. Autonom. Agent. Multi-agent Syst. 1 (1), 7–38.
Kato, S., Tsugawa, S., Tokuda, K., Matsui, T., Fujii, H., 2002. Vehicle control algorithms for cooperative driving with automated vehicles and intervehicle communications. IEEE Trans. Intell. Transp. Syst. 3 (3), 155–161.
Klein, I., Ben-Elia, E., 2016. Emergence of cooperation in congested road networks using ICT and future and emerging technologies: a game-based review. Transport. Res. C: Emerg. Technol. 72, 10–28.
Mahajan, N., Hegyi, A., Hoogendoorn, S.P., van Arem, B., 2017. Performance analysis of a decentralised routing strategy for intelligent vehicles under stochastic traffic conditions. In: Proceedings of the 96th Annual Meeting of the Transportation Research Board, Washington, D.C., United States.
Mahmassani, H.S., Jayakrishnan, R., 1991. System performance and user response under real-time information in a congested traffic corridor. Transport. Res. A: General 25 (5), 293–307.

Messmer, A., Papageorgiou, M., Mackenzie, N., 1998. Automatic control of variable message signs in the interurban scottish highway network. Transport. Res. C: Emerg. Technol. 6 (3), 173–187.
Pang, G.K.H., Takahashi, K., Yokota, T., Takenaga, H., 1999. Adaptive route selection for dynamic route guidance system based on fuzzy-neural approaches. IEEE Trans. Veh. Technol. 48 (6), 2028–2041.
Papageorgiou, M., 1990. Dynamic modeling, assignment, and route guidance in traffic networks. Transport. Res. B: Methodol. 24 (6), 471–495.
Papageorgiou, M., Diakaki, C., Nikolos, I., Ntousakis, I., Papamichail, I., Roncoli, C., 2015. Freeway traffic management in presence of vehicle automation and communication systems (VACS). In: Meyer, G., Beiker, S. (Eds.), Road Vehicle Automation. Lecture Notes in Mobility, vol. 2. Springer International Publishing, Cham, pp. 205–214 ISBN 978-3-319-19078-5.
Pavlis, Y., Papageorgiou, M., 1999. Simple decentralized feedback strategies for route guidance in traffic networks. Transport. Sci. 33 (3), 264–278.
Shladover, S.E., 2017. Connected and automated vehicle systems: introduction and overview. J. Intell. Transport. Syst. 1–11.
Wahle, J., Annen, O., Schuster, C., Neubert, L., Schreckenberg, M., 2001. A dynamic route guidance system based on real traffic data. Eur. J. Oper. Res. 131 (2), 302–308.
Wang, Y., Papageorgiou, M., Messmer, A., 2001. Feedback and iterative routing strategies for freeway networks. In: Proceedings of the 2001 IEEE International Conference on Control Applications (CCA'01). IEEE, pp. 1162–1167.
Wang, Y., Papageorgiou, M., Messmer, A., 2003. Predictive feedback routing control strategy for freeway network traffic. Transport. Res. Rec.: J. Transport. Res. Board (1856), 62–73.
Wang, Y., Papageorgiou, M., Sarros, G., Knibbe, W., 2006. Feedback route guidance applied to a large-scale express ring road. Transport. Res. Rec.: J. Transport. Res. Board (1965), 79–88.
Wardrop, J.G., 1952. Some theoretical aspects of road traffic research. Proce. Inst. Civil Eng. 1 (3), 325–362.
Weyns, D., Holvoet, T., Helleboogh, A., 2007. Anticipatory vehicle routing using delegate multi-agent systems. In: 2007 IEEE Intelligent Transportation Systems Conference. IEEE, pp. 87–93.